



Full Length Article

# Novel thermochemical fracturing: A breakthrough in sustainable and efficient enhanced geothermal systems (EGS)

Ahmed Al-Ghamdi<sup>a</sup>, Amjed Hassan<sup>b,\*</sup>, Mohamed Mahmoud<sup>a,\*\*</sup>, Talal Al-Shafloot<sup>a</sup>

<sup>a</sup> Department of Petroleum Engineering, College of Petroleum Engineering & Geosciences, King Fahd University of Petroleum & Minerals, Dhahran, 31261, Saudi Arabia

<sup>b</sup> Center for Integrative Petroleum Research (CIPR), College of Petroleum Engineering & Geosciences, King Fahd University of Petroleum & Minerals, Dhahran, 31261, Saudi Arabia

## ARTICLE INFO

### Article history:

Received 24 December 2024

Received in revised form

27 May 2025

Accepted 4 July 2025

### Keywords:

Energy sustainability  
Enhanced geothermal systems  
Thermochemical fluids  
Fracturing treatment  
Novel method

## ABSTRACT

Enhanced geothermal systems (EGS) are crucial for accessing earth's vast geothermal potential, particularly in low-permeability formations. However, conventional EGS stimulation via hydraulic fracturing often entails high operational costs, substantial water consumption, potential environmental impacts, and risks of induced seismicity. This study presents a novel thermochemical fracturing approach to enhance EGS performance and sustainability while addressing these limitations. The in-situ exothermic reaction of sodium nitrite ( $\text{NaNO}_2$ ) and ammonium chloride ( $\text{NH}_4\text{Cl}$ ) was applied to a 12-inch carbonate rock sample. A specialized core flooding apparatus enabled real-time evaluation of temperature profiles, permeability, and heat transfer enhancements. The thermochemical stimulation increased permeability by 109% (from 19.01 to 39.70 mD) and enhanced heat transfer by 530%. These improvements stem from an extensive micro-fracture network generated by high-pressure nitrogen gas pulses, contrasting with larger planar fractures from hydraulic fracturing. Notably, this was achieved with only a 3.3% increase in porosity, indicating preserved rock integrity. The exothermic reaction prevented core cooling during ambient-temperature stimulation fluid injection, avoiding thermal shock. The thermochemical stimulation primarily generates nitrogen gas ( $\text{N}_2$ ) and a brine solution as byproducts. The generated  $\text{N}_2$  offers the additional benefit of providing well lifting energy, simplifying flowback operations. The novel application of thermochemical stimulation in EGS represents a promising, eco-friendly, and operationally efficient alternative to conventional EGS stimulation techniques.

© 2025 Southwest Petroleum University. Publishing services by Elsevier B.V. on behalf of KeAi Communications Co. Ltd. This is an open access article under the CC BY-NC-ND license (<http://creativecommons.org/licenses/by-nc-nd/4.0/>).

## 1. Introduction

Geothermal energy is a renewable energy source derived from the natural heat of the Earth, which can be harnessed for electricity generation, direct heating, and other applications. This energy originates from the Earth's core and is accessible through natural geothermal reservoirs, which are areas where heat from the Earth's interior is close to the surface, as well as through enhanced geothermal systems (EGS) that artificially create fractures and improve these reservoirs' permeability [1–3].

Geothermal energy is currently utilized in 32 countries worldwide, with a combined installed capacity of 16,318 MW spread across 198 geothermal fields and 673 individual power units [2]. The United States leads in geothermal capacity, followed by Indonesia, the Philippines, and Turkey. These countries, together with others, generated 96,552 GW-h of electricity from geothermal sources in 2021, which represents 0.34% of the global electricity generation [2]. Table 1 summarizes the worldwide changes in geothermal capacity and its share of the clean energy and total energy mix.

The International Renewable Energy Agency (IRENA) and the International Geothermal Association (IGA) published in 2023 a global geothermal market and technology assessment report that describes the current state and future prospects of geothermal energy. The report identifies several key trends shaping the geothermal market, including increasing competitiveness, cross-

\* Corresponding author.

\*\* Corresponding author.

E-mail addresses: [amjed.mohammed@kfupm.edu.sa](mailto:amjed.mohammed@kfupm.edu.sa) (A. Hassan), [mmahmoud@kfupm.edu.sa](mailto:mmahmoud@kfupm.edu.sa) (M. Mahmoud).

Peer review under the responsibility of Southwest Petroleum University.

**Table 1**  
Geothermal energy share of the total energy mix from 1980 to 2023 [2].

Year	World geothermal installed capacity (MW)	Electricity generation (GW·h)			Geothermal share of	
		Geothermal	Clean energy	Total	Electricity generated through clean energy	Electricity generated from all sources
1980	2110	13,100	2,438,000	5,633,000	0.54%	0.23%
1985	4764	28,930	3,547,900	9,831,380	0.82%	0.29%
1990	5834	35,430	4,351,600	11,853,110	0.81%	0.30%
1995	6832	38,035	5,022,400	13,382,480	0.76%	0.28%
2000	7972	49,261	5,485,400	14,971,790	0.90%	0.33%
2005	8933	55,709	6,044,100	17,763,940	0.92%	0.31%
2010	10,897	67,246	6,958,800	20,938,060	0.97%	0.32%
2015	12,284	73,550	8,142,800	23,660,330	0.90%	0.31%
2020	15,414	89,587	10,186,500	26,276,910	0.88%	0.34%
2023	16,318	96,552	11,143,100	28,254,250	0.87%	0.34%

industry synergies, and expanded applications [4]. Advancements in technology and supportive government policies have led to a steady decline in geothermal energy costs, making it increasingly competitive with other renewable and fossil fuel sources. The report also highlights several barriers hindering the widespread deployment of geothermal energy. High upfront costs, including exploration, drilling, and infrastructure development. Additionally, conventional geothermal resources are predominantly found in regions with significant tectonic activity, such as volcanic areas and plate boundaries.

The geological limitations to conventional geothermal systems where the presence of high permeability and hot reservoirs are available, spurred the exploration and development of EGS. EGS technology aims to overcome the limitations of conventional systems by creating artificial reservoirs in hot dry rock formations. This is achieved by injecting fluids at pressures above the breakdown pressure to “frack” the rock and artificially enhance permeability, allowing for commercial flow rates to be achieved. The appeal of EGS is in its potential to expand the reach of geothermal energy beyond traditionally viable regions, thereby increasing the global accessibility of this renewable resource. EGS emerged from the hot dry rock (HDR) concept, first implemented at Fenton Hill in 1977 [5]. This technology aims to harness geothermal energy from hot dry rock formations lacking the natural permeability required for conventional geothermal systems.

### 1.1. Hydraulic fracturing and permeability enhancement in EGS

Hydraulic fracturing plays a crucial role in EGS by enhancing the permeability of low-permeability formations, enabling efficient fluid circulation and heat extraction [1,3,6]. The process involves injecting fluids at pressures above the rock breakdown pressure to create fractures in the rock that provide a conduit for fluid flow. Olasolo et al. [1] stated that creating conductive pathways for fluid flow is the most critical stage of the EGS project. The study also highlights that there is a clear relationship between seismic response and injected fluids during hydraulic fracturing stimulation field studies and experiments have demonstrated the effectiveness of hydraulic fracturing in various geological settings. For example, Hofmann et al. [7] highlighted that hydraulic fracturing can significantly increase productivity in low-permeability limestone geothermal reservoirs. The effectiveness of these treatments is influenced by factors such as minimum principal stress, pore pressure, permeability, porosity, and Young's modulus. In sandstone reservoirs, Zimmermann and Reinicke [8] found that the selection of high-strength proppants (HSPs) was crucial for maintaining fracture permeability under highly effective stress conditions, which is essential for long-term well productivity in EGS development.

Hydraulic fracturing, a widely used technique in both the oil and gas industries and in EGS, presents several challenges in EGS applications. Zhao et al. [9] noted the high initial costs due to the need for extensive equipment and specialized chemicals, compounded by the operational complexity and large physical equipment footprint. Hydraulic fracturing also requires substantial water volumes and utilizes various chemicals that can pose environmental risks, particularly if they contaminate surrounding groundwater supplies. Fink [10] highlighted the environmental dangers of these chemicals, especially when improperly managed, leading to potential contamination of drinking water sources. Additionally, Spellman [11] discussed the significant environmental risks, particularly the potential for aquifer contamination. Managing the flowback fluids to prevent well blockages and ensure effective geothermal energy production adds another layer of complexity.

While hydraulic fracturing is integral to the development of EGS, it also poses seismic risks. The injection of high-pressure fluids can alter the stress state within the reservoir, potentially reactivating pre-existing faults and triggering seismic events Majer et al. [12]. This induced seismicity has been observed in several EGS projects worldwide, leading to concerns about the safety and social acceptability of this technology. Notable examples include the Basel EGS project in Switzerland (2008), which experienced four earthquakes above magnitude 3 during injection, resulting in building damage, and project termination [13]. Similarly, the Pohang EGS project in South Korea (2017) induced a magnitude 5.4 earthquake, causing severe economic losses and the eventual abandonment of the project [14]. These cases underscore the importance of accurate forecasting and risk management in EGS operations. While most induced seismic events are micro-seismic and do not cause damage, the possibility of larger, damaging earthquakes cannot be ignored. The role of thermal shock and cooling effects is also complex; introducing cooler fluids into hot rock formations can cause contraction, leading to thermoelastic strain and potentially triggering slip along existing fractures ([15–17]). The interaction of these factors makes it difficult to isolate the impact of specific mechanisms, highlighting the need for comprehensive monitoring and mitigation strategies. Advances in numerical modeling, such as the work by Andrés et al. [18], which incorporates fully coupled thermo-hydro-mechanical equations, are essential for better predicting the potential for induced seismicity and evaluating the effectiveness of different injection strategies in minimizing seismic hazards.

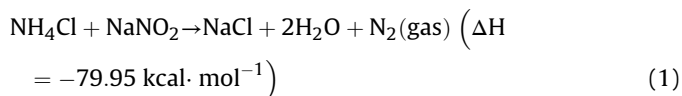
To address the challenges associated with EGS, recent research has focused on integrating laboratory experiments, numerical simulations, and field investigations. Z. Liu et al. [19] highlighted that hydraulic fracturing remains a primary focus in EGS research, with studies demonstrating its effectiveness in enhancing reservoir

permeability and heat transfer. Noteworthy, the use of thermochemical fluids as an alternative or complementary method for enhancing geothermal reservoir performance has not been explored in the literature. Unlike hydraulic fracturing, which focuses on creating large physical fractures, thermochemical fluids potentially offer a more gradual approach by leveraging exothermic reactions to generate microfractures [20–24]. These microfractures are expected to enhance permeability and increase heat transfer, while possibly mitigating some of the risks associated with conventional fracturing, such as significant seismic activity and cooling effects during treatment due to the exothermic reaction.

### 1.2. Thermochemical fluids (TC)

Chemical reactions are generally categorized as either endothermic, where they absorb heat, or exothermic, where they release heat. Thermochemical fluids fall into the latter category, being specifically designed to release significant amounts of energy in the form of heat when their chemical components react. This characteristic makes thermochemical fluids particularly useful in applications requiring energy-intensive processes, such as enhancing the productivity of subsurface reservoirs.

One of the most common and studied reactions in thermochemical fluid applications involves the interaction between ammonium chloride ( $\text{NH}_4\text{Cl}$ ) and sodium nitrite ( $\text{NaNO}_2$ ). The reaction proceeds as follows:



This reaction is highly exothermic, producing not only significant heat but also nitrogen gas and brine (a mixture of water and sodium chloride). The environmental friendliness of this reaction lies in its byproducts, which are naturally occurring substances within subsurface formations. The nitrogen gas produced can potentially contribute to the overall effectiveness of the thermochemical process by aiding in fluid displacement or further fracturing of the reservoir rock.

To optimize the effectiveness of thermochemical fluids, particularly in conditions where the in-situ temperature is not sufficient to drive the reaction, accelerants such as acids are often introduced. The presence of an acid lowers the pH, which can significantly speed up the reaction rate, ensuring that the exothermic reaction occurs at a desirable pace for the specific application [21,22,25]. This flexibility in reaction control makes thermochemical fluids a versatile tool in the field of reservoir stimulation, particularly in challenging environments where traditional methods may fall short [26,27]. Additionally, acids can enhance permeability by dissolving the rock matrix and help maintain open fractures by etching the surface, preventing closure under stress [28].

In this work, a mixture of 5% acetic acid (table vinegar) with thermochemicals will be utilized. Specifically, two solutions will be prepared: one containing 2 M concentration ammonium chloride mixed with 5% acetic acid, and the other containing 2 M concentration sodium nitrite. The use of acetic acid will not only accelerate the reaction by lowering the pH but also contribute to increasing permeability by dissolving the rock matrix and maintaining open fractures through surface etching. The reaction of acetic acid follows Eq. (2):



Thermochemical fluids are proving to be a valuable method for enhancing productivity in unconventional reservoirs like tight

sandstones, limestones, and shales. Research, including studies by Tariq et al. and A. Hassan et al. [29], demonstrates their effectiveness in reducing breakdown pressure and improving gas productivity through the creation of microfractures induced by exothermic reactions. These studies highlight up to a 69% reduction in breakdown pressure and notable increases in permeability. Further investigations into thermochemical acid fracturing, as explored by Tariq et al. in shale formations like the Eagle Ford shale, show sustained fracture permeability under high closure stresses. Amjed M Hassan et al. [30] have shown that optimizing injection strategies can lead to a significant, up to 502% increase in absolute permeability and reductions in capillary pressure.

### 1.3. Reaction kinetics of thermochemical fluids

The kinetics of the  $\text{NH}_4\text{Cl}$  and  $\text{NaNO}_2$  fluids used in this study are extensively documented in the literature [31–33]. Al-Taq et al. [34] showed that the reaction rate of  $\text{NH}_4\text{Cl}$  and  $\text{NaNO}_2$  follows the following equation as Eq. (3):

$$\frac{dc}{dt} = K[\text{NaNO}_2]^{0.97}[\text{NH}_4\text{Cl}]^{1.48} = -7.66 \times 10^{11} C_0^{2.45} e^{\frac{-91.44 \text{ kJ/mol}}{RT}} \quad (3)$$

where  $\frac{dc}{dt}$  is the rate of change of concentration of the reactants over time,  $K$  is the reaction rate constant,  $C_0$  is the initial equimolar concentration of  $\text{NH}_4\text{Cl}$  and  $\text{NaNO}_2$ ,  $R$  is the ideal gas constant ( $8.314 \text{ J} \cdot \text{mol}^{-1} \cdot \text{K}^{-1}$ ), and  $T$  is the absolute temperature (K).

The activation energy of 91.44 kJ/mol indicates a strong dependence on temperature, consistent with Arrhenius behavior. As the reservoir temperature increases, the exponential term  $e^{\frac{-91.44 \text{ kJ/mol}}{RT}}$  dominates, significantly accelerating the reaction rate. This is particularly useful for EGS where the temperature is extremely high, making the reaction highly efficient. Moreover, Al-Taq et al. [34] reported that the reaction order with respect to  $\text{NH}_4\text{Cl}$  is 1.48, higher than that for  $\text{NaNO}_2$  (0.97), which they attribute to the dual activation effect. Ammonium chloride, being a weak acid, lowers the pH of the reaction environment and catalyzes the reaction alongside thermal activation. This dual mechanism implies that systems with excess  $\text{NH}_4\text{Cl}$ , or operated at slightly acidic pH, experience faster reaction kinetics and higher nitrogen/heat output, which is favorable for EGS stimulation applications.

Moreover, the quantitative impact of temperature–pressure coupling on reaction kinetics was investigated. Both system temperature and pressure were found to significantly influence the thermochemical reaction rate. The progression of reactant conversion was monitored over time under varying initial temperatures and pressures. For instance, increasing the initial temperature from 40 to 75 °C can reduce the time required to reach the peak temperature from 500 to 350 seconds, corresponding to a 42% increase in the reaction rate. Similarly, elevating the initial system pressure accelerated the thermochemical reaction rate by approximately 23%. Further details on the influence of temperature–pressure interactions on thermochemical treatment can be found in Hassan et al. [28].

### 1.4. Comparison of thermochemical, hydraulic, and acid fracturing for EGS applications

The thermochemical treatment can overcome the common challenges associated with the conventional fracturing methods, such as hydraulic and acid fracturing. Hydraulic fracturing is commonly utilized in both conventional hydrocarbon extraction

and enhanced geothermal systems, yet its application in EGS comes with distinct challenges. As noted by Zhao et al. [9], the technique involves high initial costs due to the need for extensive equipment and specialized chemical additives, alongside a substantial operational footprint. Furthermore, it requires large quantities of water and chemical agents, which pose significant environmental risks if they infiltrate nearby groundwater systems. Fink [10] highlighted the potential for such chemicals to contaminate drinking water when not properly handled. Likewise, Spellman [11] emphasized the risk of aquifer pollution as a key environmental concern. Beyond these issues, the management of flowback fluids, which is very critical for preventing well obstruction and maintaining effective heat extraction, can add an additional level of technical difficulty in geothermal operations.

Nevertheless, hydraulic fracturing has been the cornerstone technology for unlocking hydrocarbon production from ultra-low-permeability shales, and its success naturally encouraged its adoption for permeability enhancement in unconventional geothermal targets. The process entails injecting fluid above the rock’s breakdown pressure to create fractures and then sustaining their conductivity either mechanically, by proppant emplacement (proppant- or “prop-” fracturing), or chemically, by acid etching

(acid fracturing). Proppant size, shape, and strength govern long-term conductivity in prop-fracturing, whereas acid type, concentration, and volume control the etched-width profile in acid-fracturing. Therefore, lithology plays a crucial role in determining the appropriate fracturing method. For instance, carbonate reservoirs are well-suited to acid fracturing due to their reactive mineralogy, while silicate-rich crystalline rocks typically require proppant-assisted fracturing to maintain fracture conductivity. In contrast, matrix acidizing primarily creates wormholes that aim to bypass near-wellbore damage and is ineffective for stimulating unconventional or EGS reservoirs that demand fracture creation. Table 2 compares the three fracture-creating techniques most relevant to EGS (prop-hydraulic fracturing, acid fracturing, and thermochemical stimulation) across key technical and operational dimensions.

1.5. Governing equations for heat transfer in geothermal reservoirs

The efficiency of geothermal reservoirs is primarily governed by the processes of heat transfer and fluid flow through porous and fractured rock formations. The optimization of these processes is crucial for enhancing energy extraction, and hydraulic fracturing

**Table 2**  
Comparative summary of stimulation techniques for EGS [35–38]

Parameter	Hydraulic fracturing	Acid fracturing	Thermochemical stimulation
Primary mechanism	High-pressure fluid exceeds rock breakdown pressure, creating fractures; conductivity sustained by proppant pack.	High-pressure acid injection initiates fractures; etched fracture surfaces maintain conductivity.	In-situ exothermic reaction produces high N <sub>2</sub> pressure pulses that generate a micro-fracture network; weak acid can be co-injected to etch fracture faces.
Formation suitability	Broad range of unconventional lithologies (shale, granite, limestone).	Primarily unconventional carbonate formations.	Unconventional formations where mild acid reactivity is acceptable; readily adaptable to other lithologies.
Fracture type/geometry created	Large planar propped fractures that can link with the natural fracture network.	Planar fractures with etched surfaces may develop wormholes or follow existing fractures.	Dense and spatially localized micro-fracture system.
Permeability enhancement	Orders-of-magnitude enhancement when proppant pack quality and fracture geometry are optimized; field-proven.	Orders-of-magnitude enhancement in carbonates; field-proven.	Laboratory studies report order-of-magnitude enhancement; extensive field validation still needed.
Fluid system	High water volumes (or CO <sub>2</sub> /other bases) plus gels, proppants (sand/ceramics), and chemical additives (friction reducers, biocides, surfactants).	Acid blends (HCl, acetic, organics) with inhibitors, chemical diverting agents, and mutual solvents.	Separate NaNO <sub>2</sub> and NH <sub>4</sub> Cl solutions, triggered with 5% acetic acid (mixed with NH <sub>4</sub> Cl); no proppant.
Operational aspects	Very high injection rates and pressures; large surface footprint for pumps, water, and proppant logistics; significant flowback handling.	Similar footprint to hydraulic fracturing for storage, mixing, and pumping. Additionally, requires corrosion-resistant tubulars and careful rate control, especially at high temperatures.	Smaller surface footprint; injection pressure is below breakdown pressure; N <sub>2</sub> generation aids post-treatment lift and cleanup; primary reaction products are N <sub>2</sub> and NaCl brine.
Formation/well damage risks	Proppant wash-out, embedment/crushing, gel/polymer residue, and clay swelling.	Secondary precipitates, corrosion products, fines creation, non-uniform dissolution at high temperature, corrosion, and residual polymers.	Premature reaction if fluids mix in the wellbore and high pressure may stress the well completion.
Environmental considerations	Large water demand, disposal of post-stimulation fluids, and induced-seismicity risk.	Handling/transport of strong acids; neutralization and disposal of spent acid; potential corrosion and induced seismicity.	Few reactants to handle; smaller chemical footprint; products mainly N <sub>2</sub> and brine; micro-fracturing may reduce seismic risk.
Suitability for EGS	The primary method for creating EGS fracture networks.	Selective and effective in carbonate EGS with tight temperature and corrosion control.	Promising where micro-fracturing and modest etching suffice; exothermic heat and N <sub>2</sub> generation are advantages; requires pilot-scale validation.
Long-term stability considerations	Depends on proppant design, embedment, diagenesis under high pressure and temperature.	Relies on etched asperities; closure is possible if etching is uniform or asperities degrade under high pressure and temperature.	Relies on etched micro-fracture roughness; durability under cyclic geothermal stresses and geochemical exposure required further testing

has emerged as a pivotal technique to improve permeability and heat transfer in geothermal reservoirs. It is important to understand the governing equations of heat transfer to develop a better approach of to improve existing EGS methods. Heat transfer in geothermal reservoirs occurs through conduction, convection, and radiation in some cases [39,40]. Geothermal reservoirs involve complex interactions between heat transfer mechanisms within both the solid rock matrix and the fluid flowing through porous and often fractured media.

### 1.5.1. Thermal energy balance equations

The thermal energy balance for the fluid phase in a porous medium includes both conductive and convective heat transfer, along with heat exchange with the solid matrix:

$$\begin{aligned} \nabla \cdot (\varphi \bar{\kappa}_f \cdot \nabla T_f) - \nabla \cdot (\rho_f c_{p,f} T_f \mathbf{u}_f) + q_{Tf} + \gamma_{sf} (T_s - T_f) \\ = \frac{\partial}{\partial t} [\varphi \rho_f c_{v,f} T_f] \end{aligned} \quad (4)$$

Where  $\varphi$  is the porosity of the medium (dimensionless),  $\bar{\kappa}_f$  is the effective thermal conductivity tensor of the fluid phase,  $W/(m \cdot K)$ ,  $T_f$  is the temperature of the fluid,  $K$ ,  $\rho_f$  is the fluid density,  $kg/m^3$ ,  $c_{p,f}$  is the specific heat capacity of the fluid,  $J/(kg \cdot K)$ ,  $\mathbf{u}_f$  is the velocity vector of the fluid,  $m/s$ ,  $q_{Tf}$  is the internal heat source term within the fluid phase,  $W/m^3$ ,  $\gamma_{sf}$  is the heat transfer coefficient between the solid and fluid phases,  $W/(m^2 \cdot K)$ ,  $T_s$  is the temperature of the solid matrix,  $K$ , and  $\frac{\partial}{\partial t} [\varphi \rho_f c_{v,f} T_f]$  represents the rate of change of thermal energy in the fluid phase,  $J/(m^3 \cdot s)$ .

The convective term is  $-\nabla \cdot (\rho_f c_{p,f} T_f \mathbf{u}_f)$  and the conductive term is  $\nabla \cdot (\varphi \bar{\kappa}_f \cdot \nabla T_f)$ . The thermal energy balance for the solid phase accounts for conductive heat transfer and heat exchange with the fluid, but lacks a convective term since the matrix is a rigid body, see Eq. (5):

$$\nabla \cdot ((1 - \varphi) \bar{\kappa}_s \cdot \nabla T_s) + q_{Ts} + \gamma_{sf} (T_f - T_s) = \frac{\partial}{\partial t} [(1 - \varphi) \rho_s c_{v,s} T_s] \quad (5)$$

where  $(1 - \varphi)$  is the fraction of the volume occupied by the solid matrix (dimensionless),  $\bar{\kappa}_s$  is the effective thermal conductivity tensor of the solid matrix,  $W/(m \cdot K)$ ,  $T_s$  is the temperature of the solid,  $K$ ,  $\rho_s$  is the solid density ( $kg/m^3$ ),  $c_{v,s}$  is the specific heat capacity of the solid matrix,  $J/(kg \cdot K)$ ,  $q_{Ts}$  is the internal heat source term within the solid matrix,  $W/m^3$ ,  $\gamma_{sf} (T_f - T_s)$  represents the heat exchange between the fluid and solid phases,  $W/m^3$ , and  $\frac{\partial}{\partial t} [(1 - \varphi) \rho_s c_{v,s} T_s]$  represents the rate of change of thermal energy in the solid phase  $J/(m^3 \cdot s)$ .

### 1.5.2. Hydraulic fracturing and its impact on heat transfer

One of the primary effects of hydraulic fracturing is the increase in fluid flow rates within the reservoir, which directly affects the velocity term  $\mathbf{u}_f$  in the convective heat transfer equation. By creating new fractures and expanding existing pathways, hydraulic fracturing increases the overall permeability of the reservoir, allowing fluid to flow more freely and at higher velocities through the rock matrix. This increase in fluid velocity enhances the convective heat transfer term  $-\nabla \cdot (\rho_f c_{p,f} T_f \mathbf{u}_f)$  in the thermal energy balance for the fluid phase. In addition to improving

convective heat transfer, hydraulic fracturing also enhances conductive heat transfer by increasing the heat transfer coefficient  $\gamma_{sf}$  between the fluid and the solid matrix surfaces. The creation of fractures exposes more rock surface to the fluid. This increased exposure enhances the heat transfer coefficient, allowing for more effective heat transfer between the rock and fluid. Additionally, if acid is injected into the fractures, it can further increase the surface roughness through acid etching. This process creates additional micro-roughness on the rock surfaces, further enhancing the heat transfer coefficient by increasing the contact area and turbulence at the fluid-solid interface.

## 2. Experimental set-up and procedures

In this work, the conducted experiments were designed to evaluate the impact of thermochemical fluids on the permeability, porosity, and heat transfer capabilities of carbonate formations. The procedure was divided into three phases: pre-treatment, treatment, and post-treatment.

### 2.1. Phase 1: pre-treatment

In the pre-treatment phase, the initial properties of the carbonate samples from Indiana limestone formations were determined. The core dimensions were 12 inches in length and 1.5 inches in diameter. Porosity was measured using a helium porosimeter, which accurately determines pore volume by displacing helium gas within the core. Permeability was measured by flowing 3 wt% KCl brine at constant rates of 2, 4, and 6 mL/min until pressure stabilization was achieved. The pressure data obtained from these flows along with the core dimensions were used in the Darcy equation to calculate permeability. Throughout these measurements, a backpressure of 580 psig was maintained to ensure the core was fully saturated with liquid under positive pore pressure, thereby ensuring accurate readings. A confining pressure of 1800 psig was applied during all experiments to simulate subsurface stress conditions. For the heat transfer measurements, the core holder, equipped with eight thermocouples connected to a Keysight 34970A data acquisition system, was stabilized at a temperature of 95 °C, and maintained by a heating jacket set at 200 °C. The heat flow was recorded at a steady state of 2 mL/min for 1 h, with temperature data logged at a 1-s scan rate to capture the thermal profile accurately.

### 2.2. Phase 2: thermochemical treatment

The treatment phase involved the preparation and injection of thermochemical solutions into the core, followed by monitoring of pressure and temperature profiles. Two solutions were prepared: a 2-M thermochemical solution containing 5% acetic acid, and a 2-M sodium nitrite solution. The total treatment volume of 1.5 pore volumes (approximately 90 mL) was injected in three cycles, as previous studies [28] have shown that multiple cycles enhance permeability more effectively and are practical for field operations. Before the injection, the core holder's heating jacket temperature was lowered to 140 °C to prevent the exothermic reaction from exceeding the rubber sleeve's maximum allowable temperature of 150 °C. This adjustment brought the core temperature to a stable 76 °C before the treatment injection began. As the treatment was injected, the system was closely monitored for pressure and temperature changes, and the effluent was collected to confirm the generation of nitrogen gas and verify that the expected chemical reaction was occurring.

### 2.3. Phase 3: post-treatment

In the post-treatment phase, the core's porosity, permeability, and heat transfer characteristics were re-measured to determine the effects of the thermochemical treatment. Porosity was measured again to identify any changes in pore volume. Permeability measurements were repeated under the same conditions as in the pre-treatment phase to quantify the enhancements achieved through the treatment. Heat transfer was also reassessed by repeating the same steady-state procedure at 2 mL/min for 1 h, with the system temperature raised to match the pre-treatment conditions to ensure a consistent baseline for comparison. Additionally, CT-scan images of the core were obtained to visually inspect the internal structure and identify if any wormholes were formed. The experimental setup employed for this study is illustrated in Fig. 1.

## 3. Results and discussion

The initial properties of the carbonate sample are summarized in Table 3. To visually capture the dynamics of the thermochemical reaction, Fig. 2 illustrates the reaction in a graduated cylinder one minute after the addition of both solutions, where the first solution comprises a 2-M concentration of ammonium chloride mixed with 5% acetic acid, and the second solution contains a 2-M concentration of sodium nitrite. Also, Fig. 2 provides a view of the reaction's progression 5 min after the solutions have been mixed which shows a significant amount of nitrogen gas being generated.

### 3.1. Permeability and porosity changes

The thermochemical treatment applied to the 12-inch carbonate core resulted in a substantial increase in permeability, from 19.01 mD to 39.70 mD, reflecting a 109% improvement. This

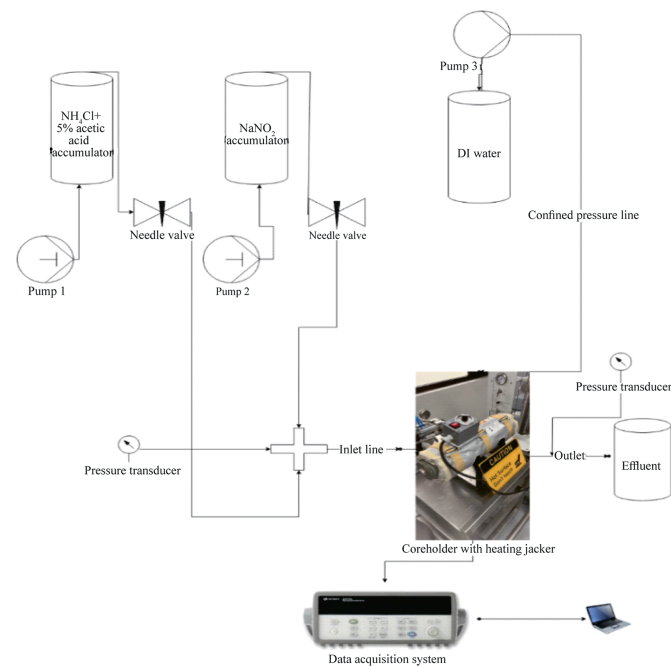


**Fig. 1.** Schematic illustration of the experimental apparatus used in the thermochemical treatment experiment.

**Table 3**

Summary of core sample dimensions, pore volume, porosity, and permeability.

Parameter	Value	Unit
Diameter	1.5	inch
Length	12.0	inch
Dry weight	773.33	g
Bulk volume	347.5	cc
Grain volume	287.02	cc
Pore volume	60.48	cc
Matrix density	2.694	g/mL
Porosity	17.40	%
Permeability	19.01	mD

significant enhancement can be attributed to the high-pressure pulses generated during the treatment, which create microfractures within the rock matrix. The porosity increased from 17.40% to 17.97%, unlike conventional hydraulic fracturing which often produces larger planar fractures, the thermochemical approach preserves the rock's integrity more effectively as shown by the minimal 3.3% increase in porosity. This smaller increase in porosity indicates that the treatment induces controlled fracturing, maintaining the structural stability of the reservoir while enhancing permeability. The minimal porosity change also suggests that the thermochemical process avoids excessive rock damage, a common issue with traditional fracturing methods. Fig. 3 shows the pressure profile during the injection with the three cycles of injection highlighted. Fig. 4 shows a photo of the collected effluent during the treatment which contains a significant amount of gas, indicating that the expected chemical reactions occurred.

### 3.2. Heat transfer enhancement

Figs. 5 and 6 compare the heat transfer and temperature profiles before and after the treatment, the post-treatment temperature profile shows significant heat exchange improvement as can be seen from the bigger gap between the two lines, representing higher withdrawal of heat from the rock by the fluid. The microfractures created during the treatment increased the exposed surface area of the rock, resulting in this additional heat exchange improvement.

In analyzing the temperature profile across the core using eight sensors, it was noted that the first three sensors, located near the inlet, are more influenced by fluid injection and connection parts. Consequently, these sensors may not accurately represent the core's true thermal conditions. Therefore, the focus was placed on the data from sensors 4 through 8, located from the center of the core until the outlet, which provides a more reliable and consistent measure of the rock's temperature response, offering a clearer picture of the treatment's effectiveness. The pre- and post-treatment temperature profiles are plotted in Fig. 7 and summarized in Table 4.

The average initial temperature in the pre-treatment and post-treatment heat transfer experiments were 96.81 °C and 96.89 °C, respectively, which is only a negligible 0.083% difference. It is critical to ensure both experiments are conducted at approximately the same initial temperature for accurate comparison. After flowing for 1 h at a steady rate of 2 mL/min, the pre-treatment and post-treatment average temperatures were 96.26 °C and 94.52 °C, respectively. Therefore, the heat transfer from the matrix to the fluid is 530 % more post-treatment, and this can be attributed to an increase in surface area available for heat exchange to take place.

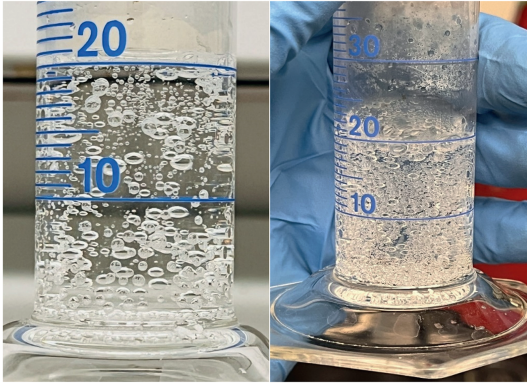


**Fig. 2.** The reaction one minute after adding the two thermochemical solutions (left) and the progression of the reaction five minutes after the initial mixing of the two solutions (right).

### 3.3. Temperature management

One of the major benefits of the thermochemical approach is its ability to maintain high reservoir temperatures, which is essential for the long-term efficiency of EGS. The exothermic reaction

during the treatment ensured that the rock temperature remained elevated, avoiding thermal shock that can occur with conventional fracturing methods, which introduce cooler fluids into the system. Fig. 8 illustrates the temperature profile during the treatment, showing the increase in rock temperature due to the exothermic reaction. This temperature stability is crucial for maintaining rock integrity and allowing operations to resume post-treatment immediately. The treatment process involved pumping thermochemical fluids in three cycles, with flow rates of 5 mL/min, 8 mL/min, and 10 mL/min. It was observed that during the first two cycles (5 mL/min and 8 mL/min), the core temperature increased, indicating an active exothermic reaction. However, at the highest flow rate of 10 mL/min, the core temperature began to decline. This suggests that the flow rate was too high for the reaction to fully occur within the core, as the fluid was moving through the system faster than the reaction could generate heat. This observation emphasizes the importance of designing the flow rates before the treatment, and also optimizing them while conducting the treatment to maximize the benefits of the exothermic reaction, ensuring effective heat generation rather than allowing the fluid to bypass the reaction process.

The structural integrity and environmental impact were investigated using the temperature profiles pre- and post-injection of thermochemical fluids. The treatment's ability to

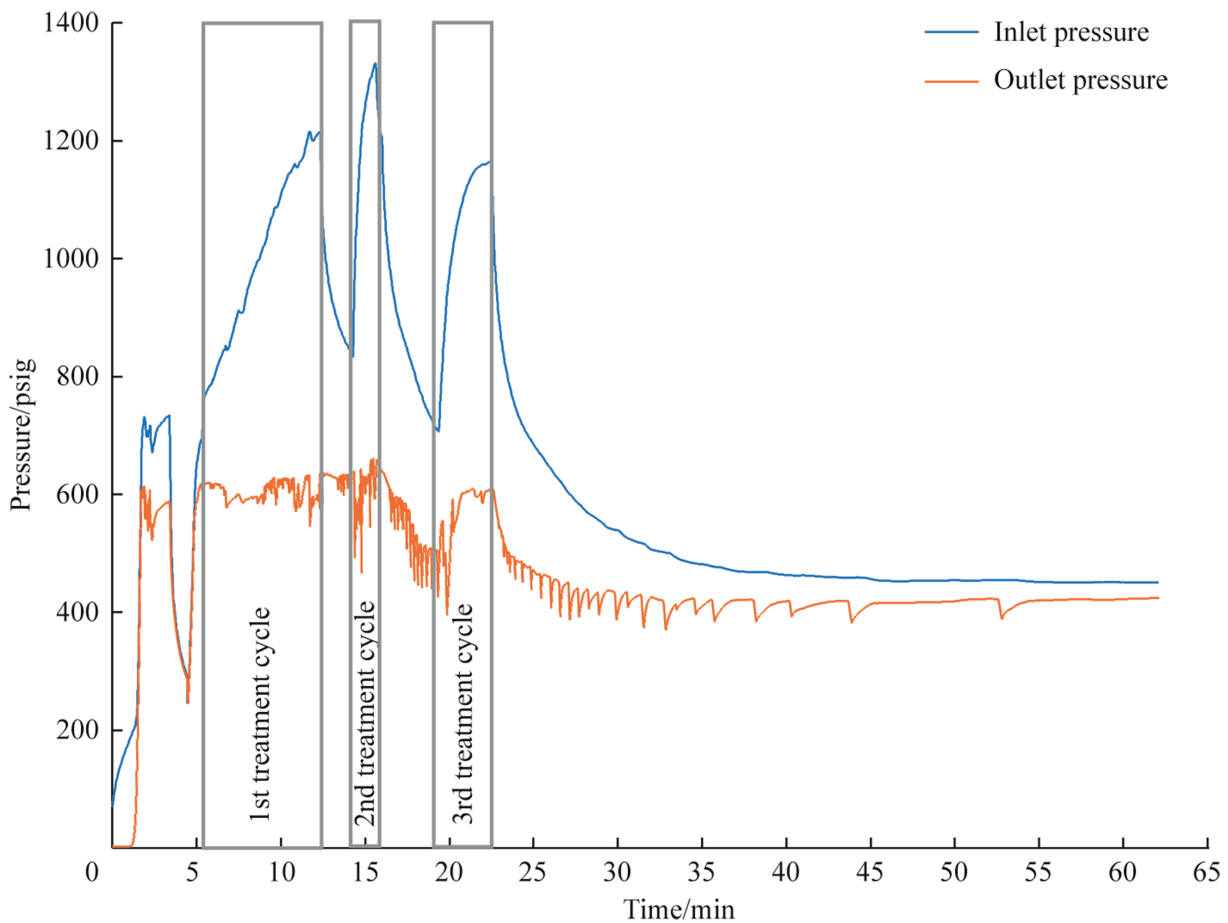


**Fig. 3.** The pressure profile during the injection of thermochemical treatment into the carbonate sample using three injection cycles.

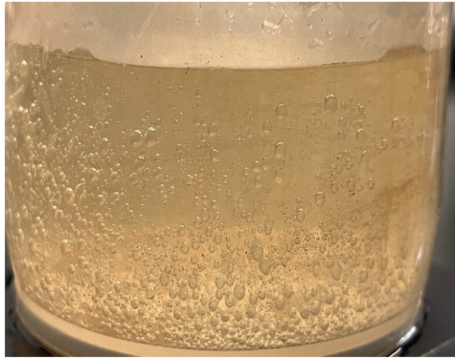


**Fig. 4.** The produced effluent from thermochemical treatment, the generated bubbles indicate reaction occurred inside the core sample.

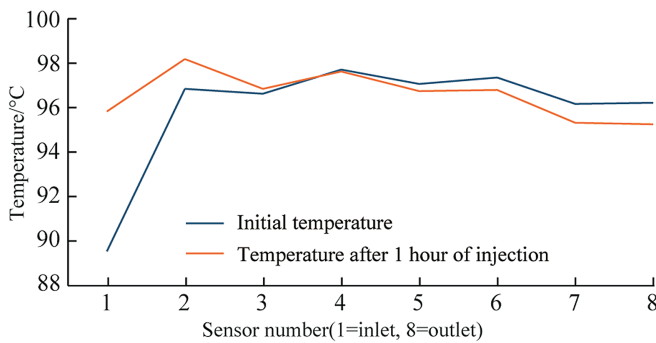


**Fig. 5.** The temperature profiles at initial conditions and after 1 h, pre-treatment, using a flow rate of 2 mL/min.

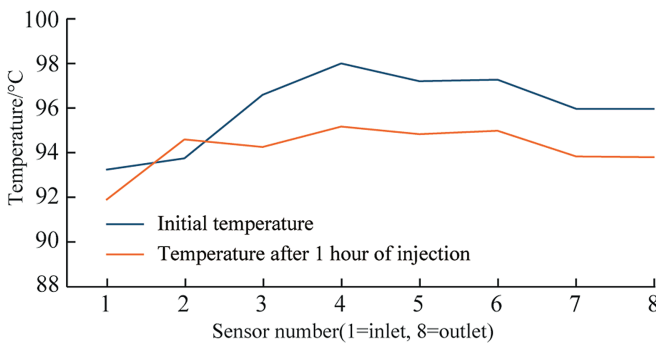


**Fig. 6.** The temperature profiles post treatment, immediately (initial temperature) and after 1 h of injection using a flow rate of 2 mL/min.

avoid cooling the rock and prevent thermal shock, combined with its minimal impact on porosity, indicates a strong preservation of structural integrity and a potential solution to mitigate induced seismic effects in EGS. Additionally, the use of environmentally friendly chemicals in the treatment process, which produces nitrogen gas and brine as byproducts, further highlights the environmental advantages of thermochemical fracturing over the chemically intensive conventional hydraulic fracturing treatment. The generated nitrogen gas not only mitigates environmental impact but also presents potential energy benefits by supplementing geothermal plant output. Moreover, nitrogen creates a low-density solution post-treatment which eliminates the need for well lifting, whereas conventional hydraulic fracturing utilizes dense and high-viscosity fluids that may require well lifting.

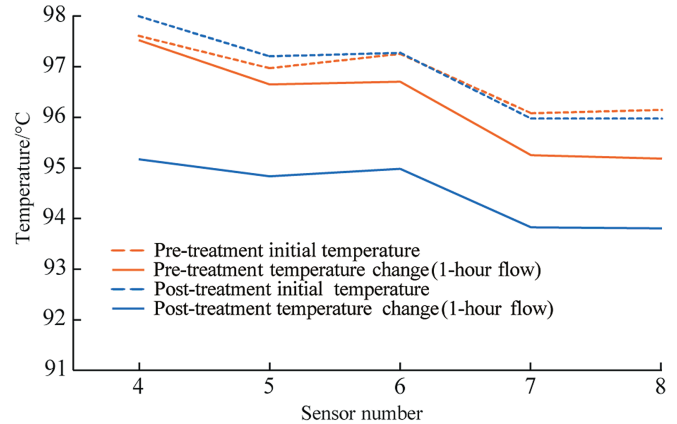


**Fig. 7.** The temperature profiles pre- and post-treatment along the core sample, using the sensors from 4 to 8.

### 3.4. CT-scan analysis

Fig. 9 provides a detailed view of these CT-scan images, which shows a wormhole development that contributes to the increase in permeability. The wormhole formation observed in the experiment was a result of using a 5% acetic acid solution mixed with 2-M ammonium chloride. Although the primary objective was to increase permeability through micro-fractures, the acetic acid, even at a low concentration, successfully created a noticeable wormhole, further enhancing permeability. If greater wormhole formation is desired, higher concentrations of acetic acid or stronger acids can be employed to amplify this effect [41], offering flexibility in treatment design based on specific reservoir needs.

### 3.5. Long-term stability considerations

While this study primarily confirms short-term improvements in permeability and heat transfer, the long-term stability of induced fractures is critical for sustained EGS performance, particularly under high-temperature and high-pressure conditions that impose significant closure stresses. In this work, 5% acetic acid was used primarily to lower the pH and trigger the thermochemical reaction, and secondarily to help sustain the openness of micro-fractures by etching their surfaces, creating roughness that resists full closure, which is an important mechanism analogous to conventional acid fracturing. Tariq et al. [42] demonstrated that acid-triggered thermochemical treatments can maintain fracture conductivity for the long term, under high closure stress due to surface etching effects. The creation of etched surfaces through acid incorporation in hydraulic fracturing is a well-established mechanism for maintaining fracture conductivity, as these etched fracture surfaces resist complete closure when subjected to in-situ stresses [43–46]. Nevertheless, to ascertain long-term efficacy, further investigation is required to determine how well the acid-etched micro-fracture surfaces sustain the fracture conductivity under high-pressure, high-temperature geothermal conditions. This should include a systematic evaluation of thermochemical stimulation using different acid types, concentrations, and volumes. More importantly, future work must also evaluate the impact of cyclic loading and geochemical interactions over extended periods while also testing with water-only and acid-only treatment as experimental controls.

**Table 4**  
The temperature readings pre- and post-treatment using the sensors from 4 to 8.

Sensor No.	Pre-treatment		Post-treatment	
	Initial temperature (°C)	Temperature after 1 h of 2 mL/min (°C)	Initial temperature (°C)	Temperature after 1 h of 2 mL/min (°C)
4	97.61	97.53	98.00	95.17
5	96.97	96.65	97.21	94.83
6	97.26	96.71	97.28	94.98
7	96.08	95.26	95.98	93.83
8	96.15	95.18	95.97	93.81
Average	96.81	96.26	96.89	94.52
Change in average temperature	-0.55		-2.36	
Enhancement in heat exchange	529.85%			

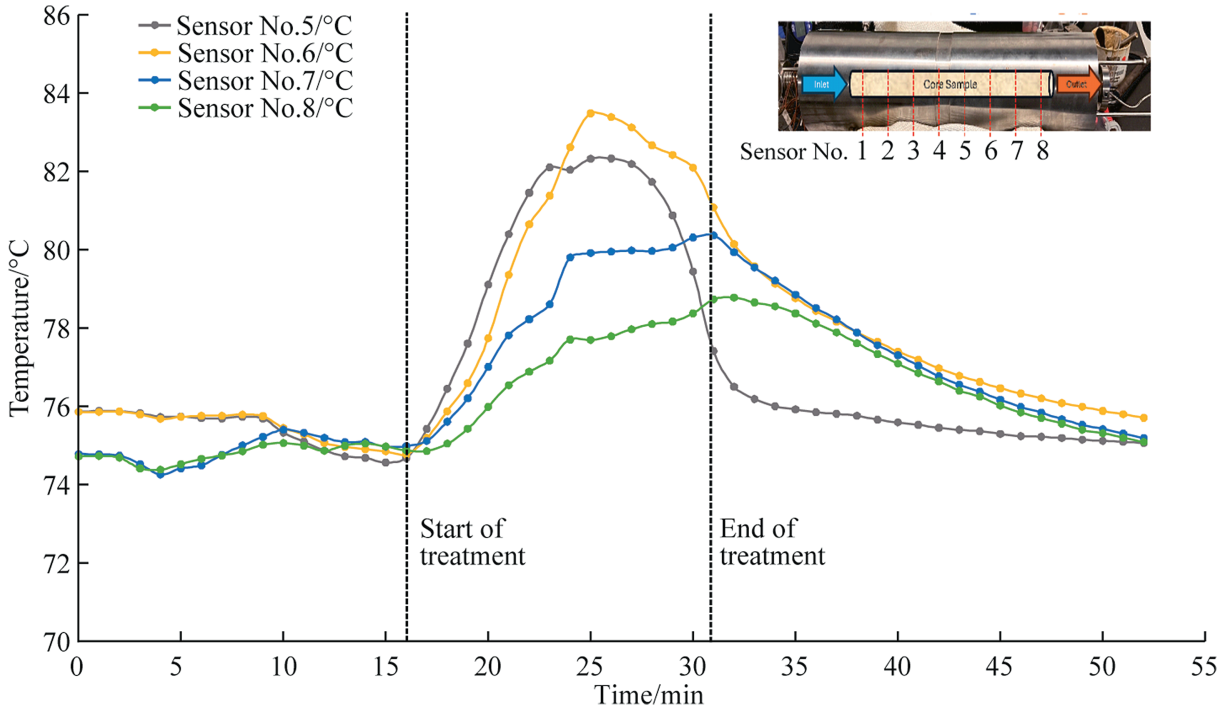


**Fig. 8.** The temperature profiles during the thermochemical treatment from the center of the core to the outlet.

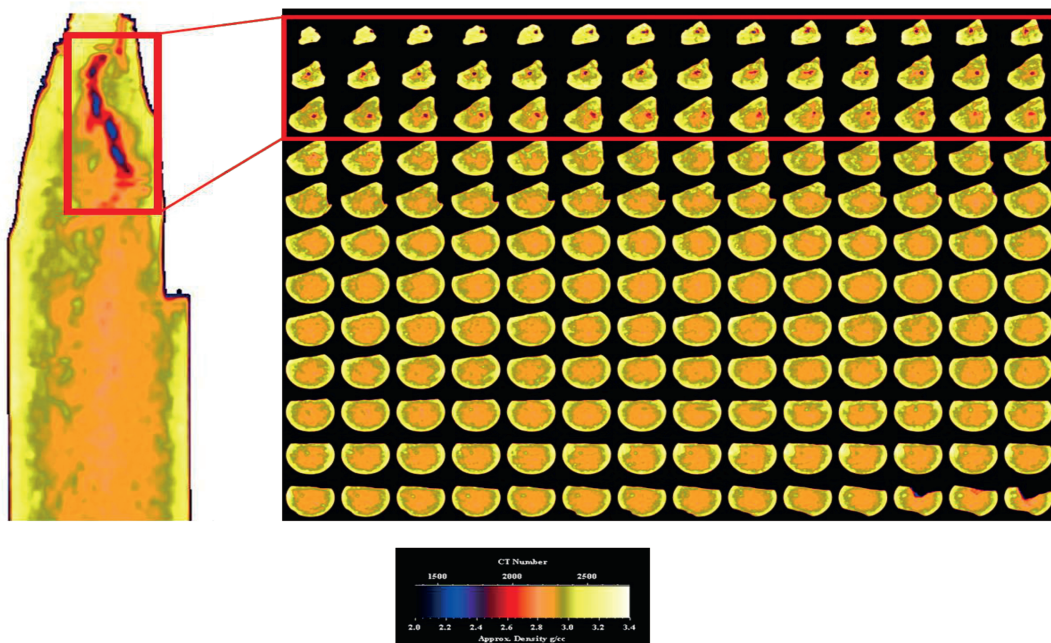


**Fig. 9.** The CT-scan images for the core sample after treatment, show wormhole development.

#### 4. Conclusions

This research has demonstrated the significant potential of thermochemical treatment as an innovative and effective approach for enhancing geothermal reservoir performance. The key findings are summarized as follows:

- (1) The thermochemical treatment applied to 12-inch carbonate cores led to a significant increase in permeability from 19.01 mD to 39.70 mD, representing a 109% improvement.
- (2) Thermochemical treatment generates high-pressure pulses that create micro-fractures while preserving the integrity of the rock. The minimal 3.3% increase in porosity observed post-treatment is significantly lower than the increases typically associated with hydraulic fracturing. This suggests that thermochemical methods may offer a safer approach, potentially reducing the risks of induced seismicity in EGS projects. Furthermore, the treatment can maintain rock integrity by avoiding thermal shock, as the exothermic reaction prevents the cooling of the rock.
- (3) The micro-fractures produced by the thermochemical treatment greatly increased the exposed surface area, resulting in a 530% enhancement in heat transfer from the rock to the fluid.
- (4) The research demonstrated the environmental advantages of thermochemical treatments, using chemicals that produce nitrogen gas and brine as byproducts. These environmentally friendly reaction products not only mitigate the ecological footprint but also offer potential energy benefits. The generated nitrogen could be harvested at the production well, supplementing the geothermal plant's output and enhancing overall efficiency.
- (5) The treatment solution generates nitrogen during the reaction, which could mitigate the need for well lifting and concerns about heavy fluids impeding post-operation flowback.
- (6) The exothermic nature of the thermochemical reaction generated additional heat, making this treatment particularly appealing for EGS applications, where maintaining high reservoir temperatures is crucial for optimal energy production.
- (7) The use of just three inexpensive and readily available components (ammonium chloride, sodium nitrite, and acetic acid) highlights the simplicity and cost-effectiveness of thermochemical treatments compared to the more complex and costly conventional hydraulic fracturing methods.

#### 5. Recommendations

Based on the findings of this study, the following recommendations are proposed to further advance the understanding and application of thermochemical treatments in EGS:

- (1) Future research should explore the use of stronger acids such as hydrochloric acid (HCl), which may offer higher dissolving power compared to acetic acid. It is also recommended to experiment with higher concentrations of acetic acid (e.g., 10%) to determine if increased concentrations will improve the treatment effectiveness.
- (2) It is recommended that future experiments test higher molar concentrations of thermochemical reagents. Increasing the concentration of the reactants may lead to

more intense chemical reactions, generating higher pressures and a denser network of micro-fractures.

- (3) It is advised to further investigate the impact on the rock structure using acoustic measurement techniques to thoroughly assess the mechanical properties post-treatment. Also, advanced imaging techniques, such as micro-CT scanning, should be explored.
- (4) Future research should also examine thermochemical treatments at elevated temperatures, such as 150 °C–200 °C. High temperatures, typical in EGS reservoirs, may intensify reaction kinetics, resulting in a denser network of micro-fractures and improved permeability and heat transfer.
- (5) Future research should investigate the long-term stability of the induced microfractures, particularly under cyclic thermal and pressure loading that mimic geothermal reservoir operation. This includes evaluating fracture closure behavior and fracture conductivity retention.
- (6) It is recommended that baseline scenarios using water-only and acid-only injections be conducted under identical experimental conditions. This will provide comparative results to quantify the incremental benefits of thermochemical stimulation relative to conventional stimulation techniques.

#### CRediT authorship contribution statement

**Ahmed Al-Ghamdi:** Methodology, Validation, Formal analysis, Writing – original draft, Investigation, Data curation. **Amjed Hassan:** Writing – review & editing, Supervision, Investigation, Data curation, Validation, Methodology, Conceptualization, Writing – original draft, Formal analysis. **Mohamed Mahmoud:** Visualization, Investigation, Writing – review & editing, Validation, Formal analysis, Conceptualization, Supervision, Data curation. **Talal Al-Shafloot:** Writing – review & editing, Data curation, Investigation, Supervision, Formal analysis, Conceptualization.

#### Declaration of competing interest

The Authors declare that they have not conflict of interest.

#### Acknowledgment

The College of Petroleum and Geoscience (CPG) at King Fahd University of Petroleum and Minerals (KFUPM) is acknowledged for the support and permission to publish this work.

#### References

- [1] P. Olasolo, M.C. Juárez, M.P. Morales, S. Damico, I.A. Liarte, Enhanced geothermal systems (EGS): a review, *Renew. Sustain. Energy Rev.* (2016), <https://doi.org/10.1016/j.rser.2015.11.031>.
- [2] L.C.A. Gutiérrez-Negrín, Evolution of worldwide geothermal power 2020–2023, *Geoth. Energy* 12 (2024), <https://doi.org/10.1186/s40517-024-00290-w>.
- [3] J. Zhang, M. Zhao, G. Wang, Effects of heat transfer fluid and boundary conditions on temperature field of enhanced geothermal system, *Petroleum* 8 (3) (2022) 436–445, <https://doi.org/10.1016/j.petlm.2021.06.006>.
- [4] I.G.A. Irena, t. Global Geothermal Market and Technology Assessmen, 2023.
- [5] K. Breede, K. Dzebisashvili, X. Liu, G. Falcone, A systematic review of enhanced (or engineered) geothermal systems: past, present and future, *Geoth. Energy* (2013), <https://doi.org/10.1186/2195-9706-1-4>.
- [6] Y. Kang, P. Li, W. Cao, M. Che, L. You, J. Liu, Z. Lai, Investigation of pore structure alteration and permeability enhancement of shale matrix by supercritical water treatment after hydraulic fracturing, *Petroleum* 10 (2) (2024) 265–274, <https://doi.org/10.1016/j.petlm.2022.05.002>.
- [7] H. Hofmann, G. Blöcher, N. Börsing, N. Maronde, N. Pastrik, G. Zimmermann, Potential for enhanced geothermal systems in low permeability limestones -

- stimulation strategies for the Western Malm karst (Bavaria), *Geothermics* 51 (2014) 351–367, <https://doi.org/10.1016/j.geothermics.2014.03.003>.
- [8] G. Zimmermann, A. Reinicke, Hydraulic stimulation of a deep sandstone reservoir to develop an Enhanced Geothermal System: laboratory and field experiments, *Geothermics* 39 (2010) 70–77, <https://doi.org/10.1016/j.geothermics.2009.12.003>.
- [9] Y. Zhao, Y. Zhang, P. He, *Hydraulic Fracturing and Rock Mechanics*, Springer, 2023, <https://doi.org/10.1007/978-981-99-2540-7>.
- [10] J. Fink, *Hydraulic Fracturing Chemicals and Fluids Technology*, Gulf Professional Publishing, 2020, <https://doi.org/10.1016/B978-0-12-822071-9.00008-6>.
- [11] F.R. Spellman, *Environmental Impacts of Hydraulic Fracturing*, CRC Press, 2012, <https://doi.org/10.1201/9781032622118>.
- [12] E.L. Majer, R. Baria, M. Stark, S. Oates, J. Bommer, B. Smith, H. Asanuma, Induced seismicity associated with Enhanced Geothermal Systems, *Geothermics* 36 (2007) 185–222, <https://doi.org/10.1016/j.geothermics.2007.03.003>.
- [13] A. Mignan, D. Landtwin, P. Kästli, B. Mena, S. Wiemer, Induced seismicity risk analysis of the 2006 Basel, Switzerland, Enhanced Geothermal System project: influence of uncertainties on risk mitigation, *Geothermics* 53 (2015) 133–146, <https://doi.org/10.1016/j.geothermics.2014.05.007>.
- [14] X. Yin, Changsheng Jiang, F. Yin, H. Zhai, Y. Zheng, H. Wu, X. Niu, Y. Zhang, Cong Jiang, J. Li, Assessment and optimization of maximum magnitude forecasting models for induced seismicity in enhanced geothermal systems: the gonghe EGS project in Qinghai, China, *Tectonophysics* 886 (2024), <https://doi.org/10.1016/j.tecto.2024.230438>.
- [15] A. Ghassemi, S. Tarasovs, A.H.-D. Cheng, A 3-D study of the effects of thermomechanical loads on fracture slip in enhanced geothermal reservoirs, *Int. J. Rock Mech. Min. Sci.* 44 (2007) 1132–1148, <https://doi.org/10.1016/j.ijrmms.2007.07.016>.
- [16] G. Izadi, D. Elsworth, Reservoir stimulation and induced seismicity: roles of fluid pressure and thermal transients on reactivated fractured networks, *Geothermics* 51 (2014) 368–379, <https://doi.org/10.1016/j.geothermics.2014.01.014>.
- [17] U. Mital, M. Hu, Y. Guglielmi, J. Brown, J. Rutqvist, Modeling injection-induced fault slip using long short-term memory networks, *J. Rock Mech. Geotech. Eng.* (2024), <https://doi.org/10.1016/j.jrmge.2024.09.006>.
- [18] S. Andrés, D. Santillán, J.C. Mosquera, L. Cueto-Felgueroso, Hydraulic stimulation of geothermal reservoirs: numerical simulation of induced seismicity and thermal decline, *Water (Basel)* 14 (2022) 3697, <https://doi.org/10.3390/w14223697>.
- [19] Z. Liu, M. Wu, H. Zhou, L. Chen, X. Wang, Performance evaluation of enhanced geothermal systems with intermittent thermal extraction for sustainable energy production, *J. Clean. Prod.* 434 (2024), <https://doi.org/10.1016/j.jclepro.2023.139954>.
- [20] Z. Tariq, M. Mahmoud, A. Abdurraheem, A. Al-Nakhli, M. BaTaweel, An experimental study to reduce the breakdown pressure of the unconventional carbonate rock by cyclic injection of thermochemical fluids, *J. Pet. Sci. Eng.* 187 (2020), <https://doi.org/10.1016/j.petrol.2019.106859>.
- [21] A. Hassan, M. Mahmoud, A. Al-Majed, M. Elsayed, A. Al-Nakhli, M. BaTaweel, Performance analysis of thermochemical fluids in removing the gas condensate from different gas formations, *J. Nat. Gas Sci. Eng.* 78 (2020), <https://doi.org/10.1016/j.jngse.2020.103333>.
- [22] I. Gomaa, M. Mahmoud, Stimulating illitic sandstone reservoirs using in-situ generated HF with the aid of thermochemicals, *J. Pet. Sci. Eng.* 190 (2020), <https://doi.org/10.1016/j.petrol.2020.107089>.
- [23] A. Mustafa, M. Mahmoud, A. Abdurraheem, Z. Tariq, A. Al-Nakhli, Improvement of petrophysical properties of tight sandstone and limestone reservoirs using thermochemical fluids, *Petrophysics – SPWLA J. Formation Evaluation and Reserv. Desc.* 61 (2020) 363–382, <https://doi.org/10.30632/PJV61N4-2020a3>.
- [24] M.S. Aljawad, M. Mahmoud, S.A. Abu-Khamsin, Mass and heat transfer of thermochemical fluids in a fractured porous medium, *Molecules* 25 (2020), <https://doi.org/10.3390/molecules25184179>.
- [25] A.H. Gowida, S.A. Abu-Khamsin, M.A. Mahmoud, M.S. Aljawad, S.F. Alafnan, Accelerated low-temperature oxidation for sand consolidation and production control, *J. Pet. Sci. Eng.* 214 (2022), <https://doi.org/10.1016/j.petrol.2022.110567>.
- [26] F.J.S. Bispo, V. Kartnaller, J. Cajaiba, pH-Based control of the kinetics and process safety of the highly exothermic reaction between ammonium chloride and sodium nitrite for flow-assurance applications, *SPE J.* 26 (2021) 3634–3642, <https://doi.org/10.2118/205389-PA>.
- [27] W. Xiuyu, C. Yuqiao, L. Chang, Z. Ya, Improved kinetic equations for a NaNO<sub>2</sub>/NH<sub>4</sub>Cl heat generating system and their implications in oil production, *Chem. Technol. Fuels Oils* 55 (2019) 623–634, <https://doi.org/10.1007/s10553-019-01075-9>.
- [28] A. Hassan, M. Abdalla, M. Mahmoud, G. Glatz, A. Al-Majed, A. Al-Nakhli, Condensate-banking removal and gas-production enhancement using thermochemical injection: a field-scale simulation, *Processes* 8 (2020) 727, <https://doi.org/10.3390/pr8060727>.
- [29] A. Hassan, M. Mahmoud, A. Al-Majed, A. Al-Nakhli, New chemical treatment for permanent removal of condensate banking from different gas reservoirs, *ACS Omega* 4 (2019) 22228–22236, <https://doi.org/10.1021/acsomega.9b03685>.
- [30] Amjed M. Hassan, M.A. Mahmoud, A.A. Al-Majed, A.R. Al-Nakhli, M. A. Bataweel, Water blockage removal and productivity index enhancement by injecting thermochemical fluids in tight sandstone formations, *J. Pet. Sci. Eng.* 182 (2019), <https://doi.org/10.1016/j.petrol.2019.106298>.
- [31] D.A. Nguyen, M.A. Iwaniw, H.S. Fogler, Kinetics and mechanism of the reaction between ammonium and nitrite ions: experimental and theoretical studies, *Chem. Eng. Sci.* 58 (2003) 4351–4362, [https://doi.org/10.1016/S0009-2509\(03\)00317-8](https://doi.org/10.1016/S0009-2509(03)00317-8).
- [32] D.A. Nguyen, H.S. Fogler, S. Chavadej, Fused chemical reactions. 2. Encapsulation: application to remediation of paraffin plugged pipelines, *Ind. Eng. Chem. Res.* 40 (2001) 5058–5065, <https://doi.org/10.1021/ie0009886>.
- [33] P. Singh, H.S. Fogler, Fused chemical reactions: the use of dispersion to delay reaction time in tubular reactors, *Ind. Eng. Chem. Res.* 37 (1998) 2203–2207, <https://doi.org/10.1021/ie9706020>.
- [34] A.A. Al-Taq, M.S. Aljawad, O.S. Alade, M. Mahmoud, A. Alrustum, Thermally activated nitrogen/heat generating reaction: a kinetic study, *ACS Omega* 8 (2023) 10139–10147, <https://doi.org/10.1021/acsomega.2c07466>.
- [35] F. Al Balushi, Q. Zhang, A. Dahi Taleghani, On the impact of proppants shape, size distribution, and friction on adaptive fracture conductivity in EGS, *Geoenergy Sci. Eng.* 241 (2024) 213115, <https://doi.org/10.1016/j.geoen.2024.213115>.
- [36] U.C. Iyare, L.P. Frash, B. K. C. M. Meng, W. Li, Y. Madenova, S.K. Peterson, M. R. Gross, M.M. Smith, K.A. Kroll, Experimental investigation of shear in granite fractures at Utah FORGE: implications for EGS reservoir stimulation, *Geothermics* 131 (2025) 103344, <https://doi.org/10.1016/j.geothermics.2025.103344>.
- [37] T. Kneafsey, P. Dobson, D. Blankenship, P. Schwering, M. White, J.P. Morris, L. Huang, T. Johnson, J. Burghardt, E. Mattson, G. Neupane, C. Strickland, H. Knox, V. Vermuel, J. Ajo-Franklin, P. Fu, W. Roggenthen, T. Doe, M. Schoenball, C. Hopp, V.R. Tribaldos, M. Ingraham, Y. Guglielmi, C. Ulrich, T. Wood, L. Frash, T. Pyatina, G. Vandine, M. Smith, R. Horne, M. McClure, A. Singh, J. Weers, M. Robertson, The EGS collab project: outcomes and lessons learned from hydraulic fracture stimulations in crystalline rock at 1.25 and 1.5 km depth, *Geothermics* 126 (2025) 103178, <https://doi.org/10.1016/j.geothermics.2024.103178>.
- [38] Z. Liu, N. Qi, P. Jiang, A. Li, X. Li, Developments of acid fracturing technology for enhanced geothermal systems: a review, *Appl. Energy* 388 (2025) 125650, <https://doi.org/10.1016/j.apenergy.2025.125650>.
- [39] M.A. Grant, P.F. Bixley, *Geothermal Reservoir Engineering*, Elsevier, 2011, <https://doi.org/10.1016/B978-0-12-383880-3.10001-0>.
- [40] A. Watson, *Geothermal Engineering Fundamentals and Applications*, Springer, 2013, <https://doi.org/10.1007/978-1-4614-8569-8>.
- [41] S. Morsy, J.J. Sheng, M.Y. Soliman, Improving hydraulic fracturing of shale formations by acidizing, in: *SPE Eastern Regional Meeting*, SPE, 2013, <https://doi.org/10.2118/165688-MS>.
- [42] Z. Tariq, M. Aljawad, M. Mahmoud, A. Abdurraheem, A.R. Al-Nakhli, Thermochemical acid fracturing of tight and unconventional rocks: experimental and modeling investigations, *J. Nat. Gas Sci. Eng.* 83 (2020), <https://doi.org/10.1016/j.jngse.2020.103606>.
- [43] A. Kamali, M. Pournik, Fracture closure and conductivity decline modeling – application in unpropped and acid etched fractures, *J. Unconv. Oil Gas Resour.* 14 (2016) 44–55, <https://doi.org/10.1016/j.juogr.2016.02.001>.
- [44] H. Liu, B. Baletabieke, G. Wang, J. Guo, F. Xia, Z. Chen, Influences of real-time acid-rock reaction heat on etched fracture dimensions during acid fracturing of carbonate reservoirs and field applications, *Heliyon* 8 (2022) e11659, <https://doi.org/10.1016/j.heliyon.2022.e11659>.
- [45] H. Jia, H. Pu, J. Li, J. Wang, X. Chen, J. Mou, B. Gao, Acid-etched fracture conductivity with in situ-generated acid in ultra-deep, high-temperature carbonate reservoirs, *Processes* 12 (2024) 1792, <https://doi.org/10.3390/pr12091792>.
- [46] P. Liu, H. Hu, X. Chen, J. Du, J. Liu, F. Liu, W. Chen, Y. Jia, The influencing parameters and improve methods of acid-etched fracture conductivity: a review, *Geoenergy Sci. Eng.* 238 (2024) 212844, <https://doi.org/10.1016/j.geoen.2024.212844>.